THE AWIATOR AIRBORNE LIDAR TURBULENCE SENSOR

N. P. Schmitt, W. Rehm, T. Pistner, P. Zeller, G. Reithmeier,
S. Stilkerich, K. Schertler, H. Diehl, H. Zinner, P. Navé

EADS Corporate Research Centre, Ottobrunn, Germany

We report on the development of a short-pulse direct measuring UV LIDAR for gust, turbulence and potentially wake vortex measurement. The system data generated are suitable for direct feed-forward coupling with the flight control system, even at cruising altitudes, where the air is devoid of aerosols. Measurable results were obtained under various flight conditions including rain, dense clouds, and clear air up to 24.000 feet.

1. Introduction

The accurate measurement of the air flow in front of an air vehicle is a very important function for modern high performance military and civil aircraft and helicopters. For military aircraft, the exact value of the true 3D airspeed vector is an essential quantity for the flight control system, especially for thrust vector control. In civil aircraft, the measurement of gust, turbulences and wake vortices and the counteraction thereof by a feed-forward flight control system would, firstly, alleviate structural loads and therefore extent the lifetime of the structure, secondly, it would considerably reduce injuries of passengers caused by turbulences and thirdly, it would provide a higher passenger comfort. It should be noted that turbulences are the leading cause of in-flight injuries [1]. Finally, the measurement and the counteraction of wake vortices could reduce the separation times during take-off and landing.
For the first type of applications coherent Doppler LIDARs have been suggested. Various US companies and institutions such as NASA, Coherent Technologies together with Boeing developed and flight-tested prototypes using IR lasers at 2 microns [2], [3]. More recently, several European programmes such as M-FLAME [4] and I-WAKE [5] have been supporting the development of similar systems, including the investigation of 1.5 micron lasers. These approaches are not suitable for feed-forward on-board detection because of the following problems:

- The coherent detection requires a narrow line width of the received signal and therefore backscatter of the laser pulses by aerosols. However, a sufficiently high aerosol density is not available in all global regions and at higher flight levels, as it is shown in fig. 1. Therefore such a system would not generate signals under all flight conditions.
- Pulsed coherent systems generate long pulses (typ. ≥ 400 ns) with low pulse repetition rates, resulting in a poor longitudinal and temporal resolution.

This sensor principle, therefore, is only suitable for long-range warning systems, but not for safety-critical applications such as feed-forward flight control.

For a safety-critical feed-forward application, the measurement scenario must meet at least the following criteria:

- A good longitudinal resolution (i.e. the thickness of the air slice ahead) of ~ ± 10 –15 m to be used by the control system
- A forward-looking measuring distance of ~ 50 – 150 m in order to ensure that the measured air flow is the one really influencing the aerodynamics of the aircraft
- A temporal resolution > 10 Hz
- In order to measure wind speeds perpendicular to the flight trajectory, the sensor must measure at various angles off the flight axis.
- The sensor must be able to produce reliable signals in the absence of aerosols; therefore it must be a molecular backscattering system.

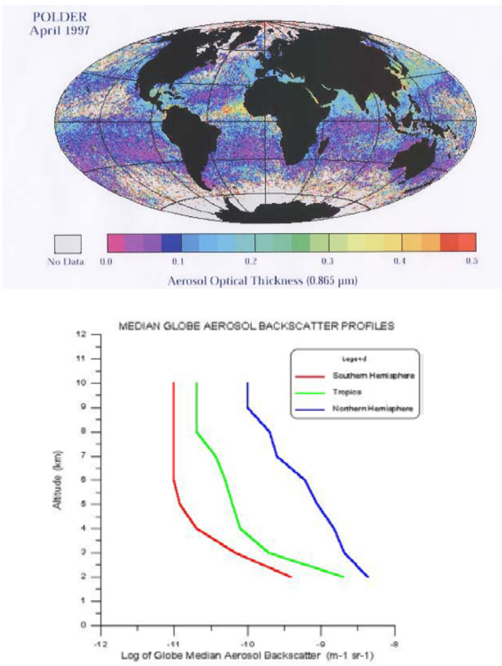

Fig. 1: Aerosol backscatter profiles. Upper: Global distribution; lower: dependence on various altitudes (from [6])

A sensor system that promises to meet these requirements is a so-called direct detection short pulse UV Doppler LIDAR. This new technology is being investigated by the US companies Ophir [7], Michigan Aerospace [8] and by European consortia, e.g. by Thales and Astrium, for space-based atmospheric missions [9] (with large integration times). Up to now, no airborne systems were shown to be suitable for a feed-forward flight control.

This contribution describes the first results achieved in flight tests with a high resolution direct measuring short pulse UV Doppler LIDAR built to generate data for later coupling with the flight control system, even at cruising altitudes, where the air is devoid of aerosols. The research has been partly funded by the European Commission within the AWIATOR project [10]. The architecture of this development is described in detail in [11].

2. Sensor principle

The preliminary requirements for the wind lidar are summarised in table 1. The sensor must be capable of measuring molecular (Rayleigh) and advantageously in addition aerosol (Mie) scattering. Fig. 2 shows the two kinds of backscattering signals.

Distance	50 - 150 m
Forward-looking time	0.2 – 0.6 s
Measurement rate	15 Hz for full vector
Longitudinal accuracy	better than ±15 m
field of view	± 10° x ± 10°
wind speed accuracy	~ ± 1 m/s

Tab.1: Preliminary requirements for the wind sensor

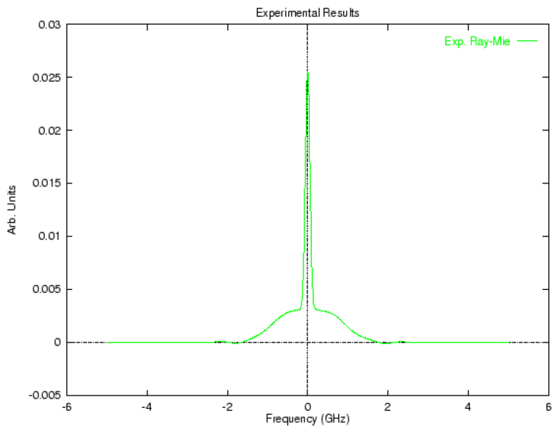

Fig. 2: **Signal (principle sketch) for Rayleigh (molecules: broad spectrum) and Mie (aerosols) scattering. In high altitudes, the Mie peak is negligible.**

The wavelength shift is measured in an interferometer, e.g. an etalon. The specified accuracy of about 1 m/s requires a frequency shift of ~ 6 MHz for the selected UV wavelength. The thermal broadening of the Rayleigh spectrum is about 600 m/s. Therefore, the frequency shift of the entire curve in fig. 2 must be measured with an accuracy of about 1/600. The shape of the spectrum also depends on parameters such as temperature, air pressure and aerosol concentration. For obtaining the full 3D wind speed vector the Doppler shift must be determined in at least 3 directions. In our case 4 directions were used for redundancy reasons (fig.3).

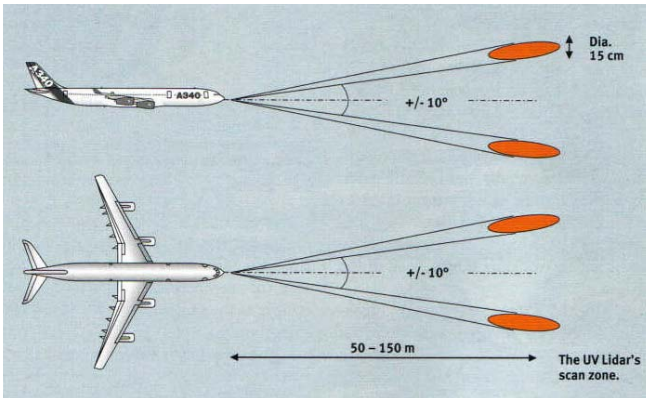

Fig. 3: Measurement geometry.

The system consists of a single-frequency frequency-tripled Nd:YAG laser, a scanning system for beam multiplexing, an optical system for beam transmission and receiving, a Fabry-Perot interferometer, an image-intensified CCD camera, a data recording and real-time data processing unit and control electronics, see fig. 4.

The LIDAR sensor is being realised in two phases. In stage 1 a (flight-worthy) system has been built capable of looking ahead 35 m and with off-line data processing, in order to study the feasibility of the principle. This was flight-tested in 2004. Stage 2 is the system that will meet the final requirements. It consists, in addition to stage 1, of an upgraded laser at 10 times the output power. It will be completed in 2005 and flight-tested in 2006.

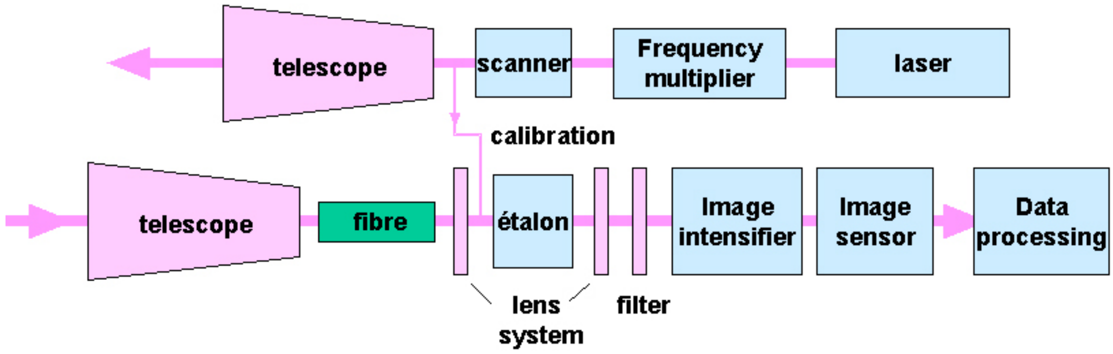

Fig 4: Sensor system architecture

The **laser** (fig. 5) is a single-frequency, third-harmonics Nd:YAG operating at 355 nm, with 300 mW for stage 1 and 3 W for stage 2. It emits pulses of ~ 10 ns width at kHz rates. It was developed by EADS, because suitable devices were not available on the market.

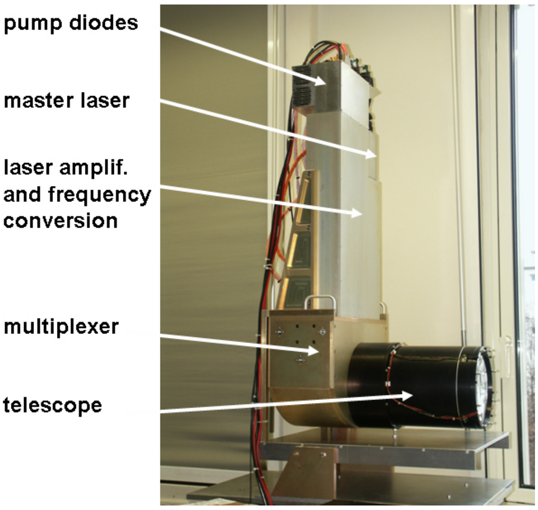

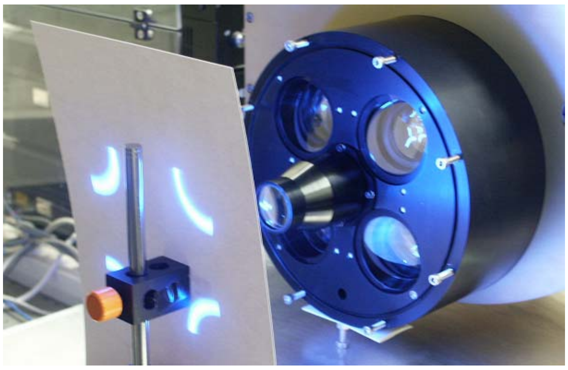

Fig. 5: Upper: laser and optical system integrated; Lower:: multiplexer

The laser beam is multiplexed in 4 directions by a scanning system (fig. 5 bottom) patented by EADS, which generates a stable focus at the four positions. A full scan is completed with 15 Hz. In the receiver path the backscattered photons are focused into four UV-fibres and de-multiplexed with a rotating mirror into one fibre that is connected to the receiver box.

The Fabry-Perot etalon was designed and manufactured by Hovemere [13]. It is capacity-stabilised and has a finesse of about 5. The Imaging System consists of a modified DiCAM Pro CCD camera with an UV sensitive microchannel plate. The sensor has 640 x 480 pixels; electronic on-chip binning is being used.

The Data Recording and Processing unit was specified by EADS; design and manufacture were contracted to Nallatech [14]. Camera data are transferred to the unit by optical transceiver/receiver interface technology. Both the recording and the processing system are based on Xilinx Virtex II FPGAs for highly parallel throughput and image processing.

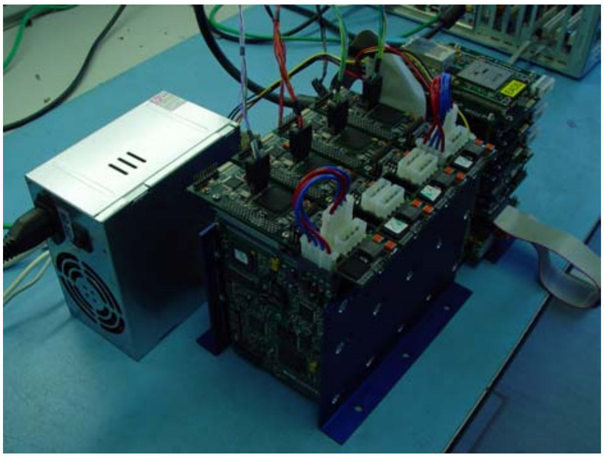

Fig. 6: Data recording/storage and processing unit

3. Theoretical model and evaluation strategy

The backscattered laser light generates, after passing through the etalon, the well-known interference pattern, called Airy function:

$$I(\lambda,\theta) = \frac{T^2}{\left(1 - R^2\right)} \frac{1}{1 + \frac{4R}{1-R} \cdot \sin^2 (\frac{\varphi}{2})}$$

with

$$\frac{\varphi}{2} = \frac{2\pi n_{gap} h \cdot \cos(\theta)}{\lambda},$$

where T and R are coefficients related to the transmission and reflection properties of the etalon, h is the gap, θ the angle of incidence, and λ the wavelength to be determined.

In practice, this function must be modified: Firstly, the thermal broadening due to the Doppler shift of the Brown´s molecular movements have to be considered, secondly the mixture of molecules and aerosols must be taken into account, and thirdly, artefacts of the optical system such as vignetting and off-centre beam axis position must be modelled. The resulting function is quite complex; in short it contains parameters describing the position of the maxima of the rings, the width of the rings dependent on the air parameters, and parameters modelling the optical flaws.
In order to obtain the desired accuracy for the backscattered wavelengths, given the expected low photon counting rates, it is not sufficient to just estimate the position of the rings by simple geometrical considerations. These parameters must be determined with sub-pixel accuracy. Therefore it is necessary to fit the above-mentioned modified Airy function with the unknown parameters to the data of the entire image plane. The system parameters, which are constant over time, are determined using the calibration signal. In order to optimise the parameter estimation process, a software simulation environment was developed, where interferograms representing various conditions could be generated. Fig. 7 shows two simulated images for various conditions, and an example of a measured and evaluated image. Note the asymmetric light distribution.

Various attempts exist in the literature to evaluate such interferograms. For real-time purposes it is desirable to transform the images into a 1d-problem, taking into account the azimuthal asymmetry. Michigan Aerospace [8] has patented an optical solution; we have found an effective digital method, suitable for highly parallel processing, which is under patent registration and will be described in a forthcoming publication.

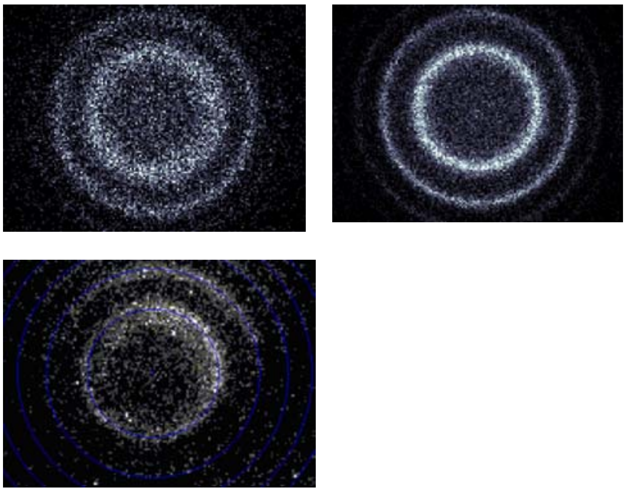

Fig. 7: Interferograms. Upper left: simulated image, low photon counts, molecular backscattering. Upper right: simulated image, high photon counts, aerosol backscattering. Lower: Measured interferogram (broad peaks) and evaluated image (circles).

4. Flight tests

The sensor was installed in the cabin of the DLR ATTAS VFW 614 test aircraft (fig. 8, fig. 9). One of the cabin windows was exchanged for a UV transmissive window with anti-reflexive coating for the laser wavelength. The symmetry axis of the sensor was tilted against the x-axis of the aircraft by β=19°, resulting in measurement directions of 61° and 81° from this axis.
Several flight tests with a duration of about 10 hours were performed. Different flight envelopes including flight levels up to 24000 feet and speeds between 120 and 240 knots were covered. The weather conditions varied from clear air to dense clouds at various altitudes.
A total of 250 Gbyte data were recorded, including flight data and system parameters.

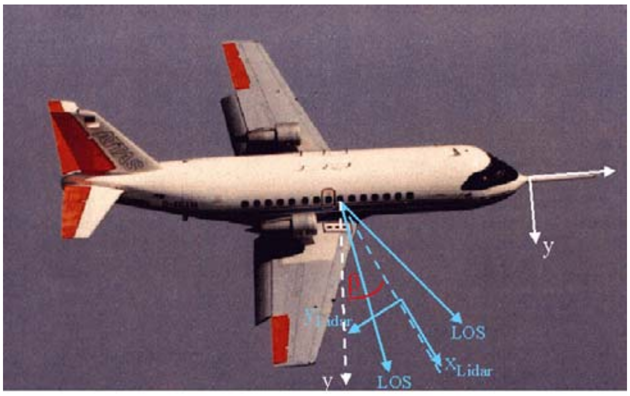

Fig. 8: Sensor installation position in ATTAS

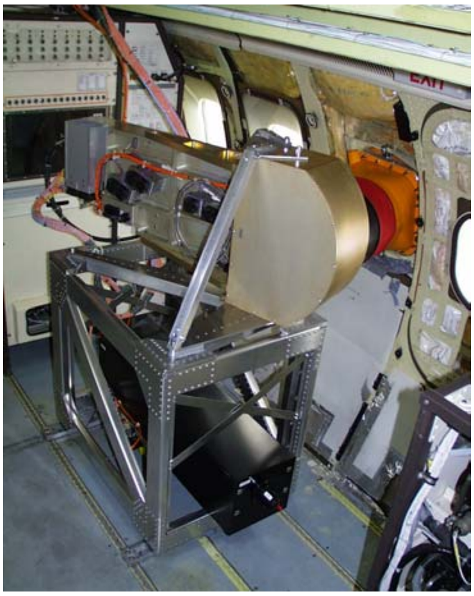

Fig. 9: Integration of the turbulence sensor in the ATTAS aircraft of DLR

5. First results and outlook

A preliminary evaluation of the data shows the following results:

- At all flight levels up to 24.000 feet interferograms could be recorded. At higher flight levels, the aerosol backscatter signal is reduced by a factor 1.000 as compared to ground level, and is therefore by a factor $5*10^{-3}$ weaker than the molecular backscatter signal. This proves that the sensor is able to perform in a pure molecular environment.
- Sensor signals were also obtained in dense clouds, where the visibility was less than 5 m (see below). The strong Mie scattering outweighed the effect of absorption of the laser beam by orders of magnitudes.
- Even in rain and ice, good sensor signals were received. Because of the gated viewing, raindrops on the window did not disturb the measurement.

Figure 10 demonstrates the LIDAR data following the curve of the aircraft onboard reference data system (nose-boom with multi-hole probe) after compensation of a constant offset.

From the preliminary evaluation the following conclusions can be drawn: The accuracy strongly depends on the photon count rate. The signal backscattered by clear air is very weak, especially in high altitudes, but still measurable. The low intensity is due to the poor interferometer throughput, which is much lower than expected. Therefore, because of the low counting rates, the specified wind speed accuracy could not yet be achieved.

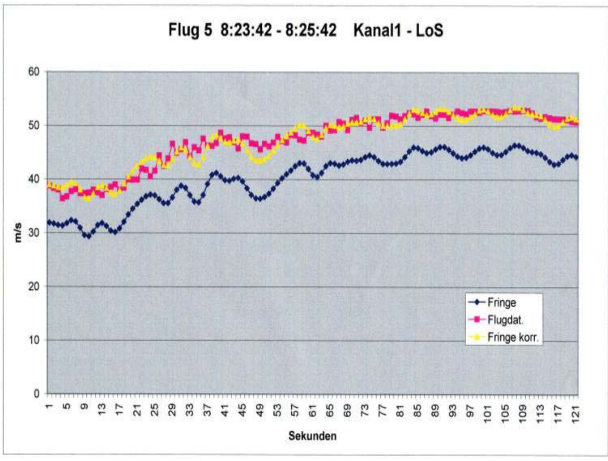

Fig.10: Flight test data from flight Nr.5:. The magenta (upper dark) curve represents the data from the aircraft´s reference system, the blue (lower dark) curve the LIDAR sensor raw data, the yellow (upper light) curve the LIDAR sensor data compensated by a constant offset. It is demonstrated that the LIDAR sensor data follow the changes measured by the aircraft´s reference system.

In Fig. 11, the flight test data are given. In direction of the abscissae, the photon counts are indicated, in the direction of the ordinate the standard deviation in m/s. The purple (dark) error bars correspond to the raw data measured in flight tests indicated at the right side of each bar, while the red (upper) and the blue (lower) dashed curve represent the theoretical limit of the standard deviation for clear air (red) and hazy layers (blue) derived from simulations. Analysing a summation of four interferograms generated the green (lighter) error bars, in contrast to the purple one from the analysis of only single interferograms, are achieved. It thus is proved that increasing the photon counts by a factor of 4 (summation of 4 frames) decreases the standard variation by the square root of 4, i.e. a factor of 2.

From the flight tests of stage 1 with the ATTAS aircraft, it can be concluded that a standard deviation of the line-of-sight air velocity of 8-12 m/s (flight 5) and 13-20 m/s (flight 6) in clear air could be achieved (depending of fight nr. with different set of parameters), 3-4 m/s (flight 5) and 5-8 m/s (flight 6) in hazy layers, and 1.8-3 m/s (flight 4) and 3.5-6 m/s (flight 6) in clouds. Taking into account a stronger laser and several improvements for the stage 2 system, which shall be flight tested in 2006 using an Airbus A340 aircraft, a standard deviation of 1.8-3 m/s and 3-4 m/s are expected in clear air conditions, and 0.7 m/s to 1.5 m/s in clouds (blue and red areas of Fig. 10) . These expectations are based on linear extrapolations of the photon count improvements, but do not take into account further reductions of systematic errors, which are indicated by vertical black arrows below the bubbles.

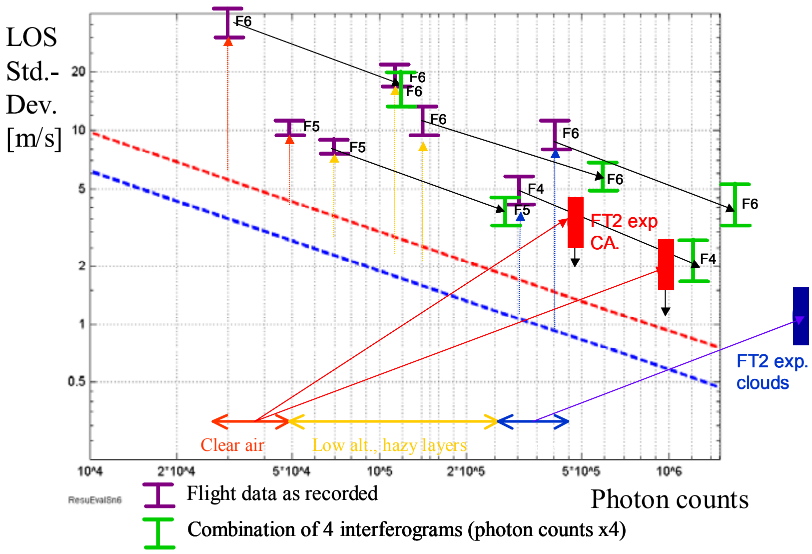

Fig. 11: Measured flight data: Line-of-sight standard deviations versus photon counts. Purple (dark) error bars: single interferogram analysis (flight number indicated right of the bar) Green (light) error bars: Summation of four interferograms. Red/blue areas: estimations for the upgraded system (higher photon counts) in flight tests stage 2 (2006) using an A340 aircraft

In a qualitative manner it could be shown that the Rayleigh/molecular short pulse Lidar works for turbulence detection, under flight test conditions up to high altitudes, in clear air and in clouds. We expect to achieve the desired performance after improvement of the evaluation methods and the upgrading of the laser to the full power.

We would like to add a remark concerning wake vortex detection. For this application, an imaging UV LIDAR system will be needed, which enables a simultaneous velocity measurement in an extended area. Scanning the beams of the turbulence sensor, several measurement volumes at different angles can be measured, allowing the caluclation of an airflow vector field. With the vector field information, wake vortices could be identified and quantified, using the same sensor system for this application as well.

In summary, forward-looking optical sensors measuring airflow, turbulences and wake vortices ahead of the aircraft, feeding the the data directly into the aircraft flight control, could improve pilot-assistance systems with automatic control, or limiting pilot commands, analogous to electronic stability program systems in automotives.

References

[1] Barnstorff, K.: Avoiding bumps in the sky. www.aero-space.nasa.gov/curevent/newsletter.com (2003)

[2] Soreide, D., et al.: Coherent LIDAR turbulence measurement for gust load alleviation. NASA Technical Memorandum 104318 (1996)

[3] Combe, H. et al.: On-board wake vortex detection. http://cerfacrs.fr/~wakenet/instru/fields/Malvern-Article.htm (2000)

[4] Phillips, M. et al.: Solid-state coherent lidar technology for space-based wind measurement. Proc. SPIE 2956 Optics in Atmospheric Propagation, Adaptive Systems, and Lidar Techniques for Remote Sensing. Devir, A. et al. (editors), 68-75 (1997)

[5] I-WAKE: Instrumentation Systems for On-board Wake Vortex and Other Hazards Detection Warning and Avoidance *CEC129*

[6] POLDER data (1997)

[7] O'Brien, M.: Rayleigh/Mie Lidar for airborne optical air data systems. www.ophir.com/rayleigh_mie_optical_air_data.htm (2002)

[8] http://www.michiganaero.com/moads/index.shtml (2001)

[9] http://www.esa.int/export/esaLP/aeolus.html (2003)

[10] www.awiator.net/project.html (2004).

[11] Zinner, H. et al.: Flight test of a short pulse UV Doppler LIDAR for Turbulence detection. In: Proc. Optro 2005 Conference Paris (May 2005); N. P. Schmitt et. al.: The AWIATOR airborne LIDAR turbulence sensor, CLEO Europe 2005 paper CH2-6-THU

[12] www.hovemere.com, Paris (May 2005)

[13] Rehm, W. et al.: Device and method for the deflec tion of a laser beam for optical measuring systems. PCT WO 2004/003626

[14] www.nallatech.com